Nonlinear Variation of Light-Pressure-Induced Multilevel Atomic Line Shifts with Vapor Pressure in Helium Spectroscopy

T. Zelevinsky[1] and G. Gabrielse[1]

[1]*Department of Physics, Harvard University, Cambridge, MA 02138*

(Dated: May 22, 2019)

Highly nonlinear dependences of ^{4}He 2^3S-2^3P lines on pressure were observed in vapor cell saturation spectroscopy. Line shifts agree with those expected from light-pressure-induced perturbation of atomic velocity distribution. In the lin⊥lin pump and probe polarization configuration, multilevel atomic structure must be taken into account. For a two-level atom, the shift magnitude is determined by the collisional time constant, but when the system has dark states there is an additional time constant due to optical pumping. The collisional and optical time constants compete, and become equal at a certain pressure p_0. Saturation signal vanishes at p_0 whereas signal due to light pressure remains. This leads to a dependence of line centers on pressure that exhibits apparently singular behavior at p_0. The $2S-2P_{J=1}$ line shift reaches the natural half width. Vapor cells may be more suitable for investigation of this effect than atomic beams since the shifts vanish at sufficiently high pressures. Two ways of controlling the shifts for the helium $2P$ fine structure measurement are discussed.

I. INTRODUCTION

Laser spectroscopy is an indispensable method for measuring optical and near-infrared transition frequencies in atoms. In particular, saturation spectroscopy [1, 2] is a two-photon technique that allows suppression of first-order Doppler shifts. It involves excitation of a single atomic velocity group by the pump laser beam and probing by the second laser beam. Monitoring the fluorescence or probe transmission signal yields line shapes limited by the natural width rather than by Doppler broadening.

We use saturation spectroscopy to carry out a precision measurement of $2^3P_{0,1,2}$ fine structure in ^{4}He. Comparison of the small ~ 2 GHz f_{12} interval to the theoretical prediction [3, 4] is a test of three-body QED, while the large ~ 30 GHz f_{01} interval combined with its theoretical expansion in α, the fine structure constant, allows to extract a value for α and compare it with other experimental determinations [5]. Recent progress on He $2P$ fine structure measurements has been reported by several groups [6, 7, 8, 9]. Hessels *et al.* [6, 7] utilized direct microwave spectroscopy of the intervals, while the experiments of Shiner and Inguscio were based on optical spectroscopy of $2S-2P$. All three groups performed measurements on metastable helium beams. Our approach of measuring the $2S-2P_J$ and $2S-2P_{J'}$ transitions and subtracting them to find the $f_{JJ'}$ intervals relies on the inherent precision of laser spectroscopy. We chose to use a vapor cell rather than an atomic beam because the cell yields a high signal-to-noise ratio, and because our results can be compared to the results of other helium experiments performed on atomic beams in order to make a judgment regarding the use of vapor cells in precision measurements.

The main function of the pump beam in saturation spectroscopy is to populate the atoms' excited state and make the sample partially transparent to the probe. However, the pump also alters the momentum state of the atoms by transferring a momentum of $\hbar k$ each time a photon is absorbed and spontaneously emitted. Thermal atomic velocity distribution attains a small deformation that can be picked up by the probe beam. This leads to frequency shifts and is critical for precision measurements. Light pressure effects have been previously predicted [10] and observed. Prentiss and Ezekiel reported fluorescence line shape asymmetries for a two-level sodium atomic beam in an intense standing-wave field [11]. Grimm and Mlynek studied shifts of probe absorption profiles for closed transitions in ytterbium vapor [12, 13, 14] due to dissipative light scattering force. Minardi and coworkers encountered light-pressure shifts for closed and open helium $2S-2P$ transitions in an atomic beam [15, 16], and explained them through scattering and dipole forces, depending on kinetic energy of the probed atoms. Their detection method used fluorescence detection rather than probe transmission which led to an additional light-intensity dependence of frequency shifts. In both cases, atoms were described as two-level systems, and line shifts reached $\sim$ 20% of the natural width Γ.

We have observed light-pressure-induced shifts of $2S-2P$ helium lines in a vapor cell and studied their manifestations with lin∥lin and lin⊥lin pump and probe polarizations. Atoms interacting with beams in lin∥lin configuration can generally be described as two-level systems with or without loss, depending on angular momentum of $2P_J$. The lin⊥lin case requires the atom to be represented as a multilevel system, and leads to line shifts of up to $\Gamma/2$. The sign of the shift in a multilevel system is opposite if angular momentum of the excited state, J_e, is smaller than that of the ground state, J_g. In addition, if $J_e \leq J_g$, optically dark states are present, and shift magnitude depends not only on the degree of velocity profile distortion, but also on the size of the saturation peak, which is the main feature of the signal. The size of this peak depends on the optical pumping time constant,

since, along with laser polarization, optical pumping determines the ground-excited state population difference that in turn controls probe transmission. When optical and collisional time constants are equal at pressure p_0, saturation signal changes sign (and therefore vanishes), while light-pressure-induced signal dominates and pulls the line center in the direction determined by the sign of the saturation peak. As a result, singularities of the type $1/(p-p_0)$ occur at p_0. These are true singularities only in the sense that the $1/(p-p_0)$ dependence holds while the splitting between the positive and negative branches of the curve is less than the half width of the line, or ~ 1 MHz for helium $2S-2P$. For larger shifts, line centers are not defined, since signal tends to vanish in the pressure region near p_0; moreover, the small-shift approximation breaks down as shifts exceed $\Gamma/2$. The discontinuity at p_0 results from competition between collisional and optical time constants and corresponds to $1/\tau \sim \Gamma/2$ where τ is the duration of coherent pumping limited by collisions.

Previous studies of light pressure relied on beam diameter as a measure of duration τ of the pump beam's interaction with the atoms. Line shifts are proportional to τ since it is a measure of deformation of the Doppler profile by light pressure. We found that varying pressure in a vapor cell gives us a very large degree of control over this systematic effect. As opposed to varying laser beam diameter, there is no uncertainty associated with the intensity profile of the pump. Instead, τ is inversely proportional to pressure p, and the proportionality constant can be found from pressure broadening of the spectral line. In fact, if an appropriate vapor pressure range is chosen, a case can be made for using vapor cells instead of atomic beams for this precision measurement. Since $\tau \propto 1/p$, light-pressure-induced shifts are negligible at higher pressures. Of course, collisions in the cell lead to line shifts [1], but if pressure is low enough for these shifts to be linear, true values of the intervals can be recovered by extrapolating line centers to zero pressure.

Our results for the lin$\perp$lin polarization arrangement are quite surprising, since they show that a highly discontinuous behavior of the absorption line center can result from a smooth variation of a continuous experimental parameter such as vapor pressure. They also illustrate the fact that extreme dependences of line centers on polarization can occur even when no dependences are expected in standard saturation spectroscopy theory.

We suggest two ways to do helium fine structure $f_{JJ'}$ measurements while reducing or eliminating the light-pressure systematic effect. The first method exploits different sensitivities to light polarization of $2S-2P_J$ and $2S-2P_{J'}$ optical transitions. A polarization arrangement can be found that makes line shifts nearly identical and subsequently they cancel upon calculation of the fine structure interval. The second method consists of resolving Zeeman sublevels of $2S$ and $2P$, and inducing optical transitions between those sublevels of $2S$ and $2P_J$, and $2S$ and $2P_{J'}$, that have the same spontaneous-decay branching ratios from $2P_J$ as from $2P_{J'}$. Light-pressure-induced shifts are then the same for both optical transitions, which leads to cancellation when fine structure intervals are computed. This method introduces additional systematic effects from magnetic shifts, but for moderate fields they are well understood and can be easily corrected for.

II. DESCRIPTION OF THE EXPERIMENT

The $2^3S_1 - 2P_{0,1,2}$ Doppler-free saturation spectroscopy of ^{4}He is performed in a pressure-variable glass cell. Spectroscopy is done with a 1083 nm diode laser, placed in an extended cavity to narrow its line width down to 0.025Γ and to allow frequency tuning. The laser beam is split into pump and probe beams that counterpropagate through the vapor cell. Pump and probe are offset by 2MHz, so they interact with atoms that are moving in the laboratory frame but with a small enough velocity that the saturation dip sits on a flat Doppler background. Pump intensity is modulated and probe transmission through the cell is detected synchronously with the pump modulation frequency. Diode laser frequency can be scanned through the resonance for all three optical transitions (the transitions are denoted simply as P_0, P_1, and P_2). Laser frequency is counted relative to the reference which is an identical diode laser locked to a transition of ^{3}He. In order to create metastable 2^3S He atoms, a coil of thick wire is wound around the vapor cell and together with a capacitor forms a circuit tuned to about 60 MHz, into which a high power resonant signal is coupled. The number of metastables created by the discharge is estimated to be roughly 1 ppm. The pressure of ground state helium in the cell is varied between 5 and 300 mTorr.

III. SUMMARY OF LIGHT-PRESSURE THEORY FOR TWO-LEVEL ATOMS

Light-pressure contribution to the probe absorption profile for two-level atoms has been worked out by Grimm and Mlynek [12, 13, 14]. The model consists of a gas of atoms with resonance frequency ω_0, line width (FWHM) Γ, and Doppler width much larger than Γ. The light field is a traveling plane wave, which is a reasonable approximation for spatially expanded laser beams.

Saturation spectroscopy is usually described in terms of the pump partly saturating the transition and thus increasing probe transmission [1]. In this case, the absorption signal is a symmetric Lorentzian with natural line width. In reality, action of the pump is not limited to saturation but also affects the momentum of the atom. Pump photons lead to cooling or heating processes that cause atomic velocities to redistribute so that they are no longer correctly described by a thermal profile. Probe transmission is sensitive to this velocity profile deformation.

Each cycle of excitation and spontaneous emission is characterized by an average momentum transfer of $\hbar k$ from the pump beam to the atom. It corresponds to the recoil frequency of $\epsilon_r = \hbar k^2/2m$. For $2S-2P$ of ^{4}He, $\epsilon_r = 2\pi \times 42$ kHz, whereas $\Gamma = 2\pi \times 1.6$ MHz. If $\epsilon_r \ll \Gamma$, light pressure can be described by the classical scattering force

$$F_s(v) = \hbar k \Gamma P_e(v),$$

where the excitation probability is

$$P_e(v) = \frac{s}{2} \frac{(\Gamma/2)^2}{k^2(v-v_2)^2 + (1+s)(\Gamma/2)^2}$$

if s is the saturation parameter and v_2 is the atomic velocity resonant with the pump. Initial velocity distribution has a Doppler profile $N_0(v)$ and evolution of $N(v)$ is described by the continuity equation [17] (y is the spatial coordinate along the laser beams)

$$\frac{\partial}{\partial t} N(v,t) + \frac{\partial}{\partial v}\left(\frac{\partial v}{\partial t} N(v,t)\right) + \frac{\partial}{\partial y}\left(\frac{\partial y}{\partial t} N(v,t)\right) = 0.$$

Since the atomic ensemble is uniform in space, $\partial/\partial y$ vanishes, and

$$\frac{\partial}{\partial t} N(v,t) = -\frac{1}{m}\frac{\partial}{\partial v}[F_s(v) N(v,t)].$$

If modification of $N(v)$ is small, we can find the first-order perturbative solution to this equation,

$$N(v,t) = N_0(v) - N_0(v_2)\frac{t}{m}\frac{\partial}{\partial v} F_s(v). \qquad (1)$$

Eq. (1) assumes that $F_s(v)$ is non-zero only for velocities in the vicinity of v_2, and that $N_0(v)$ is nearly constant in the region of non-vanishing $F_s(v)$. For a continuous laser excitation, velocity distribution reaches steady state $N(v,t) = N(v)$, and t in eq. (1) becomes τ. In our case, τ is limited by collisions of the metastable atoms with ground state helium in the cell. Making this substitution, we obtain the new velocity profile

$$N(v) = N_0(v) + \epsilon_r \tau \frac{sk(v-v_2)(\Gamma^3/2) N_0(v_2)}{[k^2(v-v_2)^2 + (1+s)(\Gamma/2)^2]^2}. \qquad (2)$$

The strength of velocity profile modification is set by dimensionless parameters $\epsilon_r\tau$ and s. The perturbative approach is justified if $\epsilon_r\tau \cdot s \ll 1$. Eq. (2) describes the dispersive kink that appears on the Doppler profile as a result of light pressure.

Absorption and dispersion of light by a medium is equivalent to multiplication of the light field by e^{-C}, where $\mathrm{Re}\,(C) = A$ is the absorption coefficient. In terms of optical response of individual velocity groups of the atoms comprising the medium,

$$A = \int_{-\infty}^{+\infty} N(v) a(v) dv.$$

Inside the integral, $a(v)$ describes the internal and $N(v)$ the external degrees of freedom of the atoms within the medium. The pump modifies not only the internal, but also the external degrees of freedom, and thus affects both $a(v)$ and $N(v)$.

For weak pump intensities, only terms of $\mathcal{O}(s^1)$ need to be kept in $N(v)$ and $a(v)$. Written as linear expansions in s,

$$a(v) = a_0(v) + s a_1(v),$$
$$N(v) = N_0(v) + s N_1(v).$$

Then

$$A = \int_{-\infty}^{+\infty} N_0(v) a_0(v) dv + s \int_{-\infty}^{+\infty} N_0(v) a_1(v) dv$$
$$+ s \int_{-\infty}^{+\infty} N_1(v) a_0(v) dv \equiv A_0 + s(A_{SAT} + A_{LP}). \qquad (3)$$

A_0 denotes response in the absence of the pump, whereas A_{SAT} and A_{LP} describe effects due to saturation and light pressure by the pump, respectively. Optical response functions $a_0(v)$ and $a_1(v)$ can be found in Refs. [12, 13, 18].

From eq. (3), saturation component of the probe absorption coefficient is calculated to be

$$A_{SAT} = -\frac{\kappa N_0(v_2)}{2} \frac{1}{k^2(v_1-v_2)^2/\Gamma^2 + 1},$$

where $\kappa \equiv 2\pi^2 n L |d|^2/\hbar$ in terms of dipole matrix element $\vec{d}$, sample length L, and atomic number density n, and v_2 and v_1 are velocities resonant with pump and probe, respectively. The light-pressure component of A can also be found from eq. (3):

$$A_{LP} = -\kappa N_0(v_2) \epsilon_r \tau \frac{k(v_2-v_1)/\Gamma}{[k^2(v_1-v_2)^2/\Gamma^2 + 1]^2}.$$

The total Doppler-free absorption, to first order in s, is

$$A_{SAT} + A_{LP} = -\kappa N_0(v_2) X(\delta), \qquad (4)$$

where

$$X(\delta) = \frac{1}{2(\delta^2+1)} + \epsilon_r \tau \frac{\delta}{(\delta^2+1)^2} \qquad (5)$$

in terms of the detuning parameter $\delta = 2(\omega - \omega_0)/\Gamma$, if ω is the pump and probe frequency. This result is derived by Grimm and Mlynek [12, 13, 14] and is presented here to facilitate further discussion.

The first term of $X(\delta)$ is the symmetric Lorentzian caused by saturation of the transition by the pump. The second term is antisymmetric in δ and has the form of a Lorentzian derivative, and is due to light pressure. Note that the strength of the light pressure effect relative to the saturation effect is independent of laser intensity at low values of s.

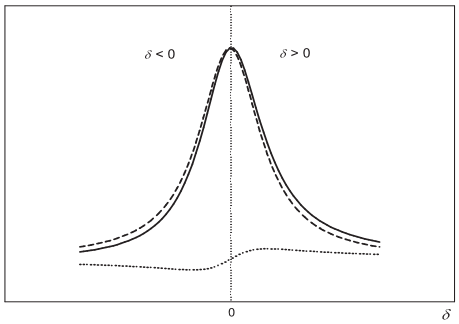

FIG. 1: Optical pressure by the pump beam effectively superimposes a dispersive component (dotted line) onto the symmetric line shape (dashed line). Here, $\epsilon_r\tau = 0.05$, and the resulting line shape (solid line) closely resembles a blue-shifted Lorentzian.

If $\epsilon_r\tau$ is a small parameter (in our experiment, $\epsilon_r\tau < 0.3$), $X(\delta)$ can be viewed as an expansion of

$$F(\delta) = \frac{1}{2}\frac{1}{(\delta - \epsilon_r\tau)^2 + 1}. \quad (6)$$

The effect of light pressure, therefore, is to shift the line center by $\delta\omega = \epsilon_r\tau\Gamma/2$. The observed line shape remains symmetrical and Lorentzian, within experimental resolution. Fig. 1 shows the shifted line for $\epsilon_r\tau = 0.05$. Interaction time τ is proportional to $1/p$, hence the line center of the measured transition appears blue-shifted by an amount inversely proportional to pressure.

Fig. 2 helps to visualize the reason for the shift. At negative detunings the probe interacts with an increased number of atoms due to the light-pressure-induced kink in the Doppler profile. Its transmission is reduced, yielding a smaller signal on the red side of the saturation peak. At positive detunings, on the other hand, the probe encounters a decreased number of atoms and its transmission is higher, leading to a larger signal on the blue side of the saturation peak. The result is the line shape in Fig. 1 (solid line).

When calculating line shapes, one must include linear pressure shifts and broadening predicted by collision theory [1, 19]. For $2S-2P$, we measured the linear pressure shift to be -1.41(2) MHz/Torr and the pressure broadening to be 25.0(2)MHz/Torr.

IV. CALCULATION OF LIGHT-PRESSURE-INDUCED SHIFTS IN HELIUM

The function $X(\delta)$ of eq. (5) precisely describes the effect of light pressure on the saturation line shape only for two-level atoms. The actual energy levels of ^{4}He contain $2J + 1$ degenerate Zeeman sublevels. They are important for optical pumping since the laser is polarized. In all three transitions we work with, 2^3S_1 is the effective

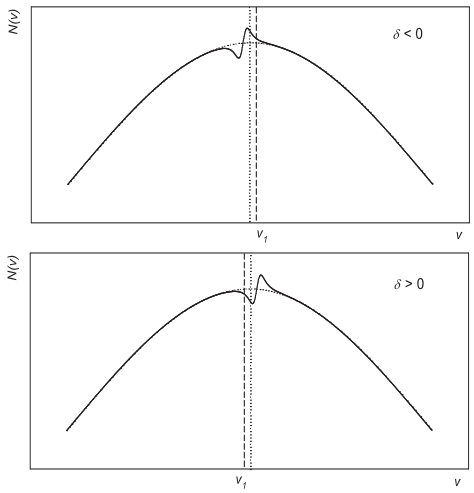

FIG. 2: Explanation of blue shift of the saturation peak. At negative detunings, the probe beam, which is resonant with atoms moving with velocity v_1, samples a larger number of atoms, yielding a lower transmission signal. At positive detunings, the probe samples fewer atoms, and its transmission is higher. The result is a blue-shifted line shape.

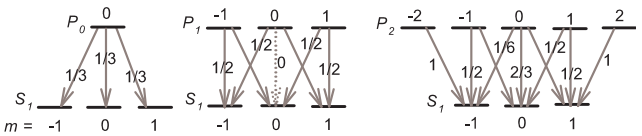

FIG. 3: Level structures and coupling coefficients for P_0, P_1, and P_2 transitions.

ground state; its sublevels are $m = \pm 1$ and $m = 0$, and it has a degeneracy of 3. Excited states 2^3P_0, 2^3P_1, and 2^3P_2 have degeneracies of 1, 3, and 5, respectively. Projections m correspond to total angular momenta J. Level structures and coupling strengths are shown in Fig. 3. In the following discussion, we take the quantization $\hat{z}$-axis to point in the direction of probe polarization, which is kept constant.

In the presence of degenerate energy levels and optical pumping, relative magnitudes of A_{SAT} and A_{LP} in eq. (4) are not constant, and therefore line shift of eq. (6) does not have a simple linear dependence on τ. For instance, if all atoms are pumped into a sublevel that does not interact with either pump or probe, increasing τ will have no further effect on line shape. In this case, a more careful investigation of time-dependent dynamics of pump-probe interaction with the atoms is necessary in order to determine the relative magnitude of the light-pressure effect.

Note that in the theoretical discussion we assumed that light pressure is due entirely to the pump. Any additional term in eq. (3) of $\mathcal{O}(s^1)$ describing velocity redistribution caused by the probe would vanish when integrated over

all velocities. This is due to the inherent experimental asymmetry between pump and probe. In the more concrete discussion of light pressure in helium below, the effect of probe on atomic velocities is included, but it only adds a minor correction to the results.

Rate equations for individual Zeeman sublevels are written in terms of velocity- and frequency-dependent unsaturated transition rates

$$R_i(\omega, kv) = \frac{s_i\gamma^3/8}{(\omega - \omega_0 \mp kv)^2 + (\gamma/2)^2}.$$

The subscript $i = 1, 2$ refers to probe and pump, respectively, $\gamma = \Gamma + \gamma_c$ is the line width that includes natural width and collisional broadening, and transition frequency ω_0 includes linear pressure shift. Doppler shift kv appears with a negative sign for the probe and a positive sign for the pump because the two beams propagate in opposite directions. Transition probability between $2S(J_g = 1; m)$ and $2P(J_e = 0, 1, 2; n)$ is proportional to R_i and to the coupling coefficient C_m^n corresponding to the appropriate J_e (Fig. 3). Time scale of population dynamics is set by the inverse of the natural line width Γ. Cross section of the probe beam's interaction with the atoms is

$$\sigma_1(\omega, kv) = \sigma_0 \frac{(\gamma/2)^2}{(\omega - \omega_0 - kv)^2 + (\gamma/2)^2}.$$

Time evolution of sublevel populations is adequately described by rate equations, taking into account pump and probe absorption and stimulated emission, as well as spontaneous decay. In order to accurately describe population dynamics of an atom undergoing elastic collisions, one needs to include re-equilibration of velocities caused by such collisions. It can be accomplished by adding terms to the rate equations that allow exchange of populations between different velocity groups. These terms can significantly complicate the problem by making rate equations nonlinear. However, a simple approximation of velocity-exchange collisions can be used instead. In order to simulate collisional velocity re-equilibration, we add the following terms to the rate equations of ground state sublevel populations:

$$\dot{g}_m^{\rm coll} = \gamma_e\Big(\sum_{n=-1}^{+1} \frac{g_n}{3} - g_m\Big),$$

where 3 is the ground state degeneracy factor. This expression would have been exact if population exchange took place between the same velocity groups of different sublevels, rather than between different velocity groups of the same sublevel. The factor γ_e is the mean elastic collision rate, proportional to the total measured collision rate γ_c. It differs slightly between the three optical transitions, since the excited state is not the same for P_0, P_1, and P_2, and although we do not explicitly include collisional effects in the excited state equations (most atoms are in the ground state), they cause effective γ_e to vary. Ground and excited state populations of sublevels with total angular momentum projection m are denoted by g_m and e_m. The quantities e_m, g_m, R_1, R_2 depend on ω, kv, s_1, and s_2. The angle of pump polarization with respect to probe polarization is θ. We exploit the symmetry $g_m = g_{-m}$ and $e_m = e_{-m}$. The stationary rate equations are

$$\Gamma \sum_{n=m-1}^{m+1} C_m^n e_n + C_m^m(R_1 + \cos^2\theta R_2)(e_m - g_m) + \sum_{n=m\pm1} \frac{1}{2} C_m^n \sin^2\theta R_2(e_n - g_m) + \dot{g}_m^{\rm coll} = 0,$$

$$\Gamma e_{m'} + C_{m'}^{m'}(R_1 + \cos^2\theta R_2)(e_{m'} - g_{m'}) + \sum_{n=m'\pm1} \frac{1}{2} C_n^{m'} \sin^2\theta R_2(e_{m'} - g_n) = 0.$$

Once the steady-state velocity-dependent sublevel populations are obtained, they are modified by light pressure as in eq. (2). This modification is proportional to τ and to dispersive functions which are defined as follows for the probe and pump:

$$D_i(\omega, kv) = \frac{s_i\epsilon_r(\omega - \omega_0 \mp kv)\gamma^3/2}{[(\omega - \omega_0 \mp kv)^2 + (1 + s_i)(\gamma/2)^2]^2}.$$

Power broadening has been included in the denominators of D_i.

The probe absorption coefficient is

$$A_1(\omega, p, s_{1,2}) = a_0 \int \Delta N(\omega, kv, p, s_{1,2})\sigma_1(\omega, kv)dv, \tag{7}$$

where a_0 is an overall pressure-dependent multiplicative factor, ΔN is the population difference between the ground and excited state sublevels coupled by the probe, and pressure p appears because of its effect on τ.

Finally, Doppler-free transmission signal observed in the experiment is

$$S(\omega, p) = A_1(\omega, p, s_1, 0) - A_1(\omega, p, s_1, s_2), \tag{8}$$

since our synchronous detection method has the effect of subtracting the signal obtained with the pump turned off.

If the functions $D_i(\omega, kv)$ are neglected, this description and specifically eq. (8) give ordinary Lorentzian saturation line shapes. Effect of light pressure as described in Sec. III is entirely included in D_i, which are used to modify the ground-excited state population difference ΔN. The resulting ΔN is inserted into eq. (7), and finally the signal line shape is computed using eq. (8). Signal profile $S(\omega, p)$ then includes the effect of light pressure as well as the ordinary saturation contribution.

For a two-level atom interacting with $\hat{z}$-polarized pump and probe, population difference which determines A_1 of eq. (7) is

$$\Delta N_{2L} = (g_0 - e_0)[1 - \tau(D_1 + D_2)].$$

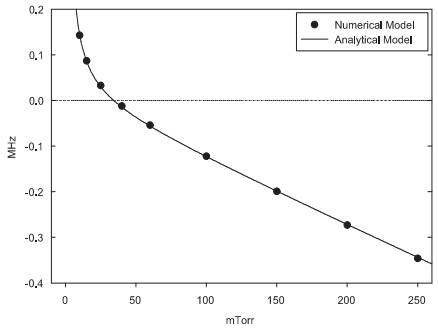

FIG. 4: Computed frequency shifts of a two-level atom due to light pressure. The approaches of Secs. III and IV give equivalent results.

Using eqs. (7) and (8), it is straightforward to compute line shapes of expected probe transmission signals and to find their frequency shifts. We use linear pressure broadening and shift values that were measured for ^{4}He. The results are shown in Fig. 4. At higher pressures, only linear pressure shift is apparent. At lower pressures, there is a shift inversely proportional to pressure. In fact, if $\tau = 1/\gamma_c$, where $\gamma_c = 0.0138\,\Gamma\,p\,/\mathrm{mTorr}$ from experiment, the shift of ω_0 due to light pressure is exactly $\delta\omega = \epsilon_r\tau\Gamma/2$, as predicted by analytical description of Sec. III and eq. (6).

For P_0, P_1, and P_2 transitions, population differences that enter the absorption coefficient (7) are found analogously to ΔN_{2L}:

$$\Delta N_{P_0} = g_0[1-\frac{\tau}{3}(D_1+\cos^2\theta D_2)] - e[1-\frac{\tau}{3}(D_1+D_2)],$$

$$\Delta N_{P_1} = (g_1-e_1)[2-\tau(D_1-\cos^2\theta D_2-\frac{1}{2}\sin^2\theta D_2)],$$

$$\Delta N_{P_2} = g_1[2-\tau(D_1-\cos^2\theta D_2-\frac{7}{6}\sin^2\theta D_2)]$$
$$+g_0[1-\tau(\frac{2}{3}D_1-\frac{2}{3}\cos^2\theta D_2-\frac{1}{2}\sin^2\theta D_2)]$$
$$-e_1[2-\tau(D_1-\cos^2\theta D_2-\frac{1}{2}\sin^2\theta D_2)]$$
$$-e_0[1-\tau(\frac{2}{3}D_1-\frac{2}{3}\cos^2\theta D_2-\frac{1}{6}\sin^2\theta D_2)].$$

V. RESULTS AND COMPARISON WITH EXPERIMENT

Including light pressure into the calculation of saturation signals yields excellent agreement with experiment. Fig. 5 (a) shows data (points) and predictions (solid curves) for all three optical transitions and the lin⊥lin pump and probe polarization configuration. At higher pressures the most prominent feature is linear pressure shift. At lower densities, velocity-equilibrating collisions become rare, and light-pressure effect is the dominant feature. All three curves exhibit significant qualitative

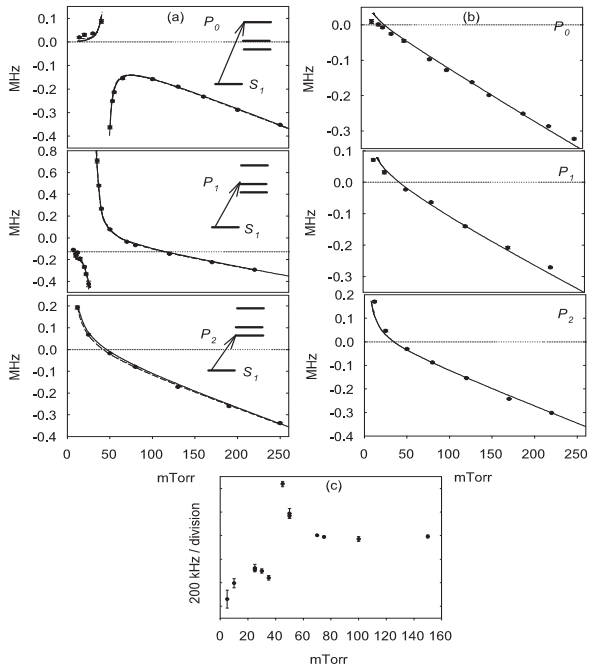

FIG. 5: (a) Line shifts for P_0, P_1, and P_2, in the lin⊥lin polarization configuration. Points are experimental values and include error bars, solid curves are calculated shifts, and dashed curves are $1/(p-p_0)$ fits to data as explained in the text. (b) Line shifts for P_0, P_1, and P_2, in the lin∥lin polarization configuration. Points are experimental values and include error bars and solid curves are calculated shifts. (c) f_{12} fine structure interval measured in the lin⊥lin configuration.

differences, and, in addition, P_0 and P_1 curves have discontinuity points. Fig. 5 (c) shows the f_{12} fine structure interval vs. pressure measured at $\theta = 90°$.

Although the curves in Fig. 5 (a) emerge from the combination of equations that describe population dynamics and velocity profile deformation by light pressure, they are not difficult to understand on an intuitive basis. The P_2 transition happens to be the simplest (refer to Fig. 3). In this case, all ground state sublevels interact with the probe, and the situation turns out to be similar to the two-level case (Fig. 4). The shift is $\epsilon_r\tau$ as in eq. (6), and $\tau \propto 1/p$.

The P_1 transition is more complicated, and pressure dependence of the line center has an effective singularity at $p_0 = 32$ mTorr. Fig. 3 shows that in this case the coupling coefficient between $m = 0$ sublevels vanishes. Therefore, if probe is $\hat{z}$-polarized, the $m = 0$ ground sublevel is a dark state into which the atom's population can be optically pumped. If the pump beam is then introduced such that polarization arrangement is lin⊥lin, the pump can restore some of the population to $m = \pm 1$ sublevels. Optical pumping is only significant at lower pressures when the optical time constant $1/\Gamma$ is close to the collisional time constant $1/\gamma_c$. As pressure is reduced, probe transmission goes from *increased* to *decreased* in

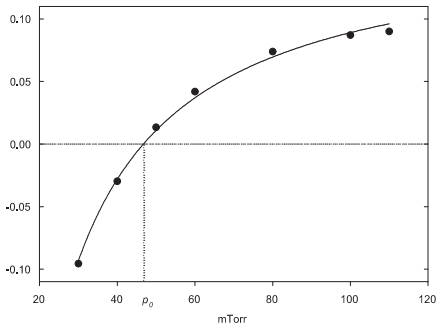

FIG. 6: Calculated ratios of P_0 signal amplitudes (lin⊥lin) to signal amplitudes of a two-level atom vs. pressure. The dependence is proportional to $1 - p_0/p$ (fitted curve).

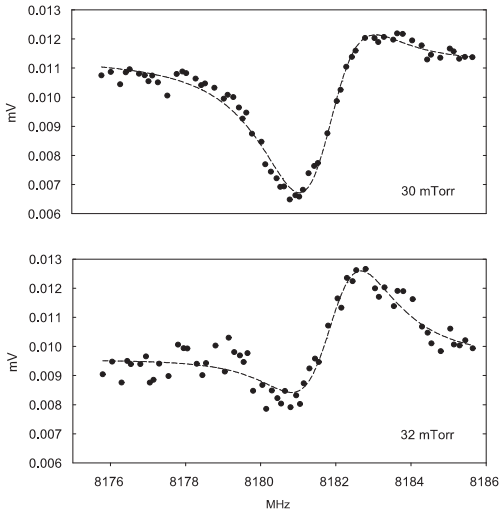

FIG. 7: Direct manifestation of light pressure creating a dispersive kink in the helium velocity distribution. The data are taken for P_1 in lin⊥lin configuration. Dashed curves are line shapes predicted by light-pressure theory.

the presence of the pump. At a special value of pressure, p_0, saturation signal amplitude vanishes, and becomes negative at lower pressures. Since the effect of scattering force is always of the same sign, the resulting line center shift changes sign at p_0. This situation is equivalent to flipping the sign of the symmetric component of the signal (dashed line in Fig. 1), while keeping the sign of the dispersive component (dotted line) unchanged. The result is a red shift of the line instead of a blue shift.

In the case of P_1, line shift can still be described by a function of the form (6), if τ is made proportional to $1/(p-p_0)$ rather than $1/p$. This can be seen from eq. (5) that describes a two-level atom. If the first term of $X(\delta)$ is multiplied by $1 - p_0/p$, line shift of eq. (6) is proportional to $1/(p - p_0)$, as long as the shift does not exceed the half width of the line (otherwise, signal-to-noise ratio becomes small and the shift so large that perturbative approximations break down). When $J_e \leq J_g$, saturation signal amplitude in the lin⊥lin configuration is indeed proportional to $1 - p_0/p$. Fig. 6 shows the calculated dependence of P_0 signal amplitude on pressure fitted to a $1 - p_0/p$ curve. The P_0 amplitude dependence on p is similar to the P_1 case, except zero crossing occurs at a slightly different pressure. Discontinuity point p_0 is the pressure at which $\gamma_c \sim \Gamma/2$. In other words, at p_0 the collisional time constant becomes approximately equal to one cycle of optical pumping which leads to the change from probe transmission to probe absorption and to discontinuous behavior of light-pressure-induced line shift.

P_0 also has dark states ($m = \pm 1$ for a $\hat{z}$-polarized probe beam), and its line center in Fig. 5 (a) shows a singularity at a pressure of 47 mTorr. The overall sign of the light-pressure-induced shift here is reversed. This is due to the fact that in the lin⊥lin configuration, probe interacts with the $m = 0$ sublevels, but pump cannot exert pressure on the $m = 0$ ground state sublevel. Therefore, probe picks up only deformation of the excited state velocity distribution, whereas in the P_1 and P_2 cases deformation of ground state distributions plays a dominant role.

In addition to theoretical predictions, Fig. 5 (a) shows fits to the data (dashed lines). The fitting function is

$$f(p) = \frac{a}{p - p_0} - 0.00141p,$$

where $p_0 = 0$ for P_2, the coefficient of the second term is the previously measured linear pressure shift, p is in mTorr, f is in MHz, and $a \propto \epsilon_r \tau$.

The theory of light-pressure shifts in a vapor cell is based on just two parameters, γ_e and τ. The velocity-equilibrating collision rate γ_e differs by $\sim$ 20% for P_0, P_1, and P_2, since it is a phenomenological constant and is affected by differences in level structure. γ_e is uniquely determined by discontinuity points, and equals $0.39\,\gamma_c$ and $0.52\,\gamma_c$ for P_0 and P_1, respectively. P_2 pressure dependence is relatively insensitive to the exact value of γ_e, and it was chosen to be $0.5\,\gamma_c$ for computational purposes. The second parameter, τ, also depends on transition, since it is the mean duration of coherent action of the pump that couples different sublevels in the three transitions. τ was found from the lin⊥lin data to be $1.8/\gamma_c$, $2.5/\gamma_c$, and $1.2/\gamma_c$ for P_0, P_1, and P_2, respectively.

The constants γ_e and τ are also expected to have a mild dependence on θ. However, they were kept unchanged for a prediction of light-pressure-induced shifts for lin∥lin polarization configuration. Qualitative agreement is very good and is shown in Fig. 5 (b). In this arrangement, P_2 line center is affected the most, since P_2 is a closed system and resembles a two-level system in both lin⊥lin and lin∥lin situations. P_1 and especially P_0 are affected less, since they are open systems in this case, optical pumping severely limits τ, and light-pressure-induced shifts cannot grow too large.

The lin⊥lin P_0 and P_1 signal quality is poor near p_0 since saturation signal amplitude vanishes at that point

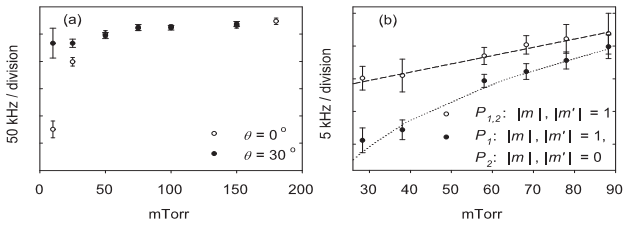

FIG. 8: (a) f_{12} fine structure interval vs. pressure at $\theta = 0°$ and $\theta = 30°$. (b) f_{12} vs. pressure measured in a magnetic field. White circles: average of $m = \pm 1 \rightarrow m' = \pm 1$ transitions. Linear slope is the pressure shift of f_{12}. Black circles: $m = \pm 1 \rightarrow m' = \pm 1$ for P_1, $m = 0 \rightarrow m' = 0$ for P_2. Aside from the pressure shift, there is a residual light-pressure-induced shift since the mean numbers of scattered photons, $\langle n \rangle$, differ for P_1 and P_2. Dotted line corresponds to theoretical pressure dependence of line shifts fitted to data with one free parameter. If this parameter is appropriately scaled, it can be used for light-pressure-induced shift correction for f_{01} and f_{02}. The scaling is determined from the difference in $\langle n \rangle$ for the optical transitions.

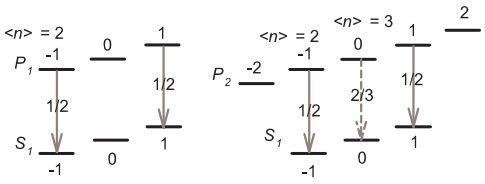

FIG. 9: f_{12} measurement unaffected by light-pressure shifts (in a magnetic field). Shifts cancel for $m = \pm 1 \rightarrow m' = \pm 1$. If instead $m = 0 \rightarrow m' = 0$ is used for P_2, shifts do not cancel since mean numbers of scattered photons, $\langle n \rangle$, are not the same. The difference between these two f_{12} measurements serves as a calibration for f_{01} and f_{02} shifts.

(Fig. 6). Therefore, line center values cannot be obtained for p_0 and the nearby pressure values. When the Lorentzian component of eq. (5) vanishes, however, the dispersive component can still be observed. When P_1 data were collected near $p_0 \simeq 31.5$ mTorr, the effect of light pressure was seen directly, as illustrated in Fig. 7. The first line shape was taken at $p < p_0$ and demonstrates a significant red shift, while the second line shape corresponds to $p > p_0$ and shows an equivalently large blue shift. The distance between the peaks is almost 2 MHz, or a full line width.

VI. CONTROLLING LIGHT-PRESSURE-INDUCED LINE SHIFTS

From Figs. 5 (a) and (b) it is evident that P_2 is much less sensitive to θ than P_0 and P_1. We found that at $\theta \simeq 30°$, the pressure curve for the P_1 shift looks qualitatively similar to the P_2 curve. The f_{12} fine structure interval is plotted vs. pressure for $\theta = 30°$ in Fig. 8 (a), and at this angle the dependence of the interval on pressure is significantly minimized.

The method of choosing the optimal θ is generally not adequate for a high precision fine structure measurement, since residual light-pressure-induced shifts remain at low pressures due to intrinsic differences between sublevel structure of the two optical transitions which leads to different degrees of velocity profile distortion. The f_{12} interval can be measured in a way that allows light-pressure-induced shifts to cancel entirely. Such a measurement is achieved by resolving Zeeman sublevels with a $\hat{z}$-directed magnetic field and measuring optical transition frequencies only between sublevels with those m-values that have the same coupling strengths for both P_1 and P_2. This implies that the scattering force affects velocity distributions in equivalent ways, and the difference $P_1 - P_2$ is free of shifts. The unique choice of optical transitions follows from considerations of coupling coefficients (Fig. 3): $m = \pm 1$ sublevels are coupled with $\hat{z}$-polarized pump and probe, as shown in Fig. 9.

f_{01} and f_{02} intervals do not allow such cancellation of light-pressure-induced shifts. However, if f_{12} is measured using the $m = 0 \rightarrow m' = 0$ transition for P_2 (Fig. 9), along with the 'clean' $m = \pm 1 \rightarrow m' = \pm 1$ result it can be used as a calibration of shifts for f_{01} and f_{02}. A comparison of the two f_{12} measurements vs. pressure is shown in Fig. 8 (b).

VII. CONCLUSION

We observed and explained a new manifestation of light-pressure-induced line shifts in ^{4}He vapor cell saturation spectroscopy. The shifts for $2S - 2P_2$ are qualitatively similar to those for two-level atoms, but $2S - 2P_0$ and $2S - 2P_1$ shifts must be explained using multiple Zeeman sublevels, and in the lin$\perp$lin pump-probe polarization configuration exhibit singularities of the form $1/(p - p_0)$ as a function of vapor pressure, as long as the shifts do not exceed $\sim \Gamma/2$. These discontinuities result from a competition of the collisional and optical pumping time constants. When the time constants are equal at p_0, the saturation contribution to the Doppler-free signal vanishes and changes sign, while the dispersive light-pressure contribution remains finite. When dark states are present, either blue shifts or red shifts are possible above p_0, depending on whether populations of ground or excited states coupled by the probe are absorbing most of the recoil. We found that vapor cells allow an easy control of this systematic effect, and demonstrated two ways to carry out precise fine structure measurements with light-pressure-induced shifts strongly suppressed.

ACKNOWLEDGMENTS

We thank C. Levy, T. Roach, N. Hermanspahn, and D. Farkas for valuable contributions to the experiment. We are also grateful to S. Ezekiel and D. Phillips for discussions and helpful suggestions. This work was supported by NSF.

[1] W. Demtröder, *Laser Spectroscopy, 3rd edition* (Springer, 2003).
[2] T. W. Hänsch and H. Walter, Rev. Mod. Phys. **71**, S242 (1999).
[3] G. W. F. Drake, Can. J. Phys. **80**, 1195 (2002).
[4] K. Pachucki and J. Sapirstein, J. Phys. B **35**, 1783 (2002).
[5] T. Kinoshita, Rep. Prog. Phys. **59**, 1459 (1996).
[6] M. C. George, L. D. Lombardi, and E. A. Hessels, Phys. Rev. Lett. **87**, 173002 (2001).
[7] C. H. Storry, M. C. George, and E. A. Hessels, Phys. Rev. Lett. **84**, 3274 (2000).
[8] J. Castillega, D. Livingston, A. Sanders, and D. Shiner, Phys. Rev. Lett. **84**, 4321 (2000).
[9] F. Minardi, G. Bianchini, P. C. Pastor, G. Giusfredi, F. S. Pavone, and M. Inguscio, Phys. Rev. Lett. **84**, 3274 (2000).
[10] A. P. Kazantsev, G. I. Surdutovich, and V. P. Yakovlev, JETP Lett. **43**, 281 (1986).
[11] M. G. Prentiss and S. Ezekiel, Phys. Rev. Lett. **56**, 46 (1986).
[12] R. Grimm, Ph.D. thesis, Swiss Federal Institute of Technology (1989).
[13] R. Grimm and J. Mlynek, Appl. Phys.B **49**, 179 (1989).
[14] R. Grimm and J. Mlynek, Phys. Rev. A **42**, 2890 (1990).
[15] F. Minardi, M. Artoni, P. Cancio, M. Inguscio, G. Giusfredi, and I. Carusotto, Phys. Rev. A **60**, 4164 (1999).
[16] M. Artoni, I. Carusotto, and F. Minardi, Phys. Rev. A **62**, 023402 (2000).
[17] V. G. Minogin and V. S. Letokhov, *Laser Light Pressure on Atoms* (Gordon and Breach, London, 1987).
[18] V. S. Letokhov and V. P. Chebotayev, *Nonlinear Laser Spectroscopy, Springer Ser. Opt. Sci. 4* (Springer, London, 1977).
[19] D. Vrinceanu, S. Kotochigova, and H. R. Sadeghpour (2003).


This figure "EnergyLevelsHe4.jpg" is available in "jpg" format from:
http://arxiv.org/ps/physics/0401075v1

This figure "ExptSetup.jpg" is available in "jpg" format from:

http://arxiv.org/ps/physics/0401075v1